

# Femtosecond Laser-Assisted Optoporation for Drug and Gene Delivery into Single Mammalian Cells

Pranav Soman<sup>1,†</sup>, Wande Zhang<sup>1,†</sup>, Aiko Umeda<sup>2,†</sup>,  
Zhiwen Jonathan Zhang<sup>2,\*</sup>, and Shaochen Chen<sup>1,\*</sup>

<sup>1</sup>Department of NanoEngineering, University of California, San Diego, 9500 Gilman Drive, Atkinson Hall, MC-0448, La Jolla, CA 92093-0448, USA

<sup>2</sup>Division of Medicinal Chemistry, College of Pharmacy, The University of Texas at Austin, 1 University Station, C0850, Austin, Texas 78712, USA

In this work, focused near-infrared (NIR) femtosecond laser pulses were used to transiently perforate the cellular membrane of targeted human embryonic kidney (HEK) cells and the uptake of extrinsic molecules into the targeted cells was observed. Various cellular responses to the laser treatments were closely analyzed to optimize several experimental parameters such as laser power, exposure time and location of laser irradiation using a membrane impermeable fluorescent dye. The optimized parameters were used to investigate the entry of a plasmid DNA encoding green fluorescent protein (GFP) into the target cells. Since laser beam with higher-than-threshold energy level will disintegrate cells, we used Matlab simulations to characterize the laser irradiance and free electron distribution caused by the femtosecond-optoporation process. The simulation results showed that the free electron distribution is much narrower than the laser irradiance, which implies that the transient perforation can even be smaller than the size of the laser focal volume. Femtosecond laser-assisted optoporation when combined with lab-on-a-chip devices can be useful in single cell-based high-throughput screening.

**Keywords:** Femtosecond Laser, Optoporation, Single-Cell Manipulation, HEK, Transfection, GFP, Matlab Simulations.

## 1. INTRODUCTION

Traffic of molecules in and out of living cells is tightly regulated by the plasma membrane. This barrier of phospholipid bilayer is generally selective against hydrophilic and the charged molecules as well as various macromolecules including nucleic acids, peptides and proteins.<sup>1</sup> Targeted and reversible permeabilization of the plasma membrane is of paramount interest in today's biology and biotechnology. For example, to analyze the behavior of drugs and substrates or inhibitors for certain enzymes or to localize cellular proteins by fluorescence-based immunocytochemistry, the delivery of the given reagents or antibodies into the cell interior is an absolute prerequisite. Ideally, these observations should be made in the intact "live" cells to harness the most reliable and biologically relevant data.<sup>17</sup> However, such real-time observations can be challenging as seen in cellular imaging, in which most of the commonly used techniques requires fixation and

detergent-based membrane permeabilization to deliver the antibodies or dyes into the cell interior.<sup>7</sup>

Transfection of the cultured mammalian cells is one of the indispensable techniques in biomedical research laboratories. Hydrophilic DNA molecules are commonly introduced into cells using either liposomal or cationic chemical delivery vehicles, viral vectors, or physical permeabilization such as electroporation.<sup>9</sup> Liposomal delivery and electroporation are sometimes also used for the injection of compounds other than nucleic acids.<sup>6</sup> These methods allow manipulations and analyses of intact cells. However, in most cases, cells are treated as a population and the produced data only represents the average of the whole group. Single-cell manipulation and analyses has been drawing attention recently since it is well accepted that there are cell-to-cell variabilities in many biological aspects, and analyses of individual cells could often provide a wealth of information.<sup>12</sup> Although microinjection has been established as a method to introduce the foreign substances into intact single cells,<sup>20</sup> the method is inefficient, time-consuming and technically very challenging. As the notion of lab-on-a-chip (LOC)<sup>12</sup> and lab-in-a-cell

\*Authors to whom correspondence should be addressed.

†These authors contributed equally.

(LIC)<sup>2</sup> emerged as devices for high throughput single cell analyses, there is an immediate need for a quick, efficient and versatile method to deliver extrinsic compounds and reagents into single cells.

Optical-poration or optoporation has recently been receiving much attention as a promising method for easy and efficient delivery of extrinsic compounds into single live cells. Femtosecond laser can produce a tiny, submicrometer-sized pore, which lasts for a fraction of a second, at a defined location on the plasma membrane of a target cell to facilitate introduction of membrane impermeable substances such as foreign DNA. Femtosecond laser has been used by several groups for a number of cell lines, reporting cell viabilities from 50% to 100% using a variety of impermeable substances.<sup>8, 10, 13–15, 18</sup>

Laser optoporation offers a number of advantages over existing techniques to deliver membrane impermeable molecules into cells:

- (1) laser optoporation is highly selective with capabilities of delivering materials into a single cell located in a cell-cluster;
- (2) this technique is compatible with standard microscopy optics, coverslip configuration, microfluidic and LOC applications;
- (3) it is a non-contact and aseptic method;
- (4) its operation requires much less technical training of researchers compared to microinjection, since the most instrumental setup allows them to simply aim at the most focused point of the laser on the cell image and shoot (“point-and-shoot”).

Single cell manipulation using the femtosecond optoporation technique could have far reaching consequences in the field of bioengineering, tissue engineering and stem cell therapy.<sup>13</sup>

There is, however, a major hurdle towards establishing the point-and-shoot cellular optoporation with femtosecond laser: the process must be optimized for each specific cell line or instrumental set-up. Several parameters such as (a) exposure time (b) laser power and (c) location of irradiation need to be characterized for the best and reproducible results. Optimization of these variables can be a daunting and time-consuming task. Also in many experiments using live cell culture, the specific cells treated with the laser have to be re-located after several hours or days of incubation to investigate the effects of genes, indicators, antibodies and other compounds introduced into the target cells.<sup>3, 13</sup> In fact, there is no standardized protocol for optoporation. Discrepancies are seen in previously reported values for laser parameters, causing difficulties in independent reproduction of the data. Most laboratories only specify the laser power and exposure time, which worked for the group, using their specific equipments and set-up. Most contemporary laser ablation studies are still conducted on systems assembled in-house based on different types of lasers and vary dramatically in their designs. Often, this

results in disagreements between groups regarding the type of instrumentation needed for a particular task.

In this work, we present for the first time a detailed systematic study on the optimization of the protocol for the femtosecond laser-assisted optoporation. As a model, we used human embryonic kidney (HEK) cell line which is one of the most commonly used cell lines in current biomedical laboratories. We employed both a membrane impermeable fluorescent dye and a plasmid DNA encoding green fluorescent protein (GFP) to analyze the entry of extrinsic molecules into the target cells and the technology's effects on the cellular biology. Characterization of laser intensity during optoporation process is important since cellular disintegration can result from laser irradiations at intensities higher than the cells' survival threshold. Therefore, we used Matlab algorithm to simulate the process of femtosecond laser ablation to better understand the laser radiation produced during the process. The behavior of the target cells after laser irradiation was extensively and thoroughly analyzed to compare various sets of parameters. By providing a protocol to systematically evaluate multiple combinations of laser parameters and cellular responses, this study could serve as a starting point for other groups to optimize their optoporation procedures for specific cell lines.

## 2. MATERIALS AND METHODS

### 2.1. Cell Culture and Preparation

All optoporation experiments were performed using 35 mm petri dishes with poly-D-lysine coated glass bottom of 10 mm diameter and 0.17 mm thickness (Model Number: P35GC-0-10-C, MatTek Corporation, Ashland, MA). A 4 × 4 square grid with each square area of about 200 μm × 200 μm was manually scratched on the bottom side (outside) of each dish using a tungsten carbide scribe. Human embryonic kidney (HEK) 293H cells were maintained in Dulbecco's Modified Eagle Media (DMEM, Invitrogen, Carlsbad, CA) with 10% v/v Fetal Bovine Serum (FBS Atlanta Biologicals, Norcross, GA) and 1X Antibiotic/Antimycotic Solution (Cellntec, Switzerland) in a humidified incubator at 37 °C with 5% CO<sub>2</sub>. Cells were seeded on the glass bottom dish with 1 mL culture medium without phenol red and grown for 48 hours to achieve 10–30% confluency before laser treatments.

### 2.2. Laser Instrumentation Set-Up

Figure 1 shows the experimental setup of the femtosecond laser-assisted optoporation. Ti:sapphire femtosecond laser (Vitesse, Coherent Inc. Santa Clara, CA) produces 100-femtosecond duration pulses with a central wavelength of 800 nm at 80 MHz frequency. The femtosecond laser beam was expanded by a homemade 2X beam expander before it was focused on the cell membrane by

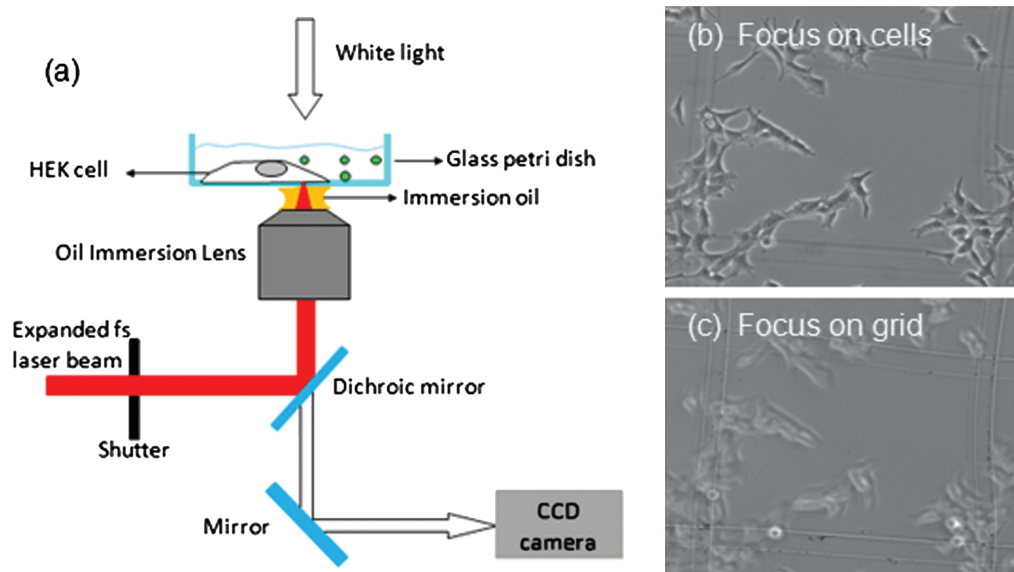


**Fig. 1.** (a) Schematic representation of the laser set-up for optoporation of targeted single HEK cell. (b) A grid was fabricated by a tungsten carbide scribe on the under-side of a glass-bottom culture dish. HEK cells were then seeded and grown to approximately 10–30% confluency. HEK cells in focus on the top side of the culture chamber. (c) Grid in focus on the underside of the culture dish.

a 100X oil-immersion objective lens (N.A. = 1.3, Fluor, Carl Zeiss MicroImaging, Inc. Thornwood, NY) which was mounted in an inverted microscope (Olympus IX81, Olympus America Inc., Center Valley, PA). Laser power was measured by a power meter (PowerMax 500D, Moletron Detector Inc. Portland, Oregon) before laser beam entered the objective lens. The power switch of the laser beam was controlled by an electrical-motorized shutter (Edmund Optics Inc. Barrington, NJ). A built-in piezoelectric step motor in the microscope controlled the vertical position of the laser focal point. The glass bottom dish containing cultured HEK cells was mounted on the stage of the microscope, and the horizontal movement of stage was actuated by two perpendicularly placed step motors (Newport Inc. Irvine, CA) with a moving resolution of 50 nm. The optoporation process was monitored *in situ* by a charge-coupled device (CCD) camera (Q-imaging; Rolera-XR; Q-16467). To find the position of laser focal point, the laser was tuned to very low energy (about 3 mW) and an empty area of the dish was irradiated. A bright spot indicating the position of laser focal point was noted on the monitor connected to the CCD camera. A marker was used to label the center of the bright spot—the focal point. Before laser optoporation, the specific area of the targeted cell was moved to the center of laser focal point. The desired laser power for optoporation of the HEK cell membrane was selected by rotating the laser beam attenuator as measured by the laser power meter. The laser exposure time of the cell was selected by programming open duration of the mechanical shutter. The term ‘targeted cell’ in this paper refers to single HEK cells at the corners of each square grid. Cells adjacent to the targeted cells were not

treated by the laser and served as the control population (Refer to Figs. 1(b, c)).

### 2.3. Optoporation Using Femtosecond Laser

SYTOX® Green nucleic acid stain (10  $\mu$ M, Invitrogen, Carlsbad, CA) was added to the culture medium before each optoporation experiment. Targeted cells were irradiated with varying laser parameters. An optical attenuator was used to adjust the laser average power in a range of 10 mW to 100 mW with 10 mW increments. The exposure time was varied from 10 ms to 100 ms with 10 ms increments. Targeted cells were re-located using the square grid and fluorescence signal was monitored for 1 hour after irradiation. Viability of the cells after laser exposure was determined by staining the non-viable cells with 0.5% Trypan Blue (Sigma-Aldrich, St. Louis, MO), 40 minutes post-laser-treatment. For each condition, three or more different cells were tested. All reported data in this work represent the results from successfully reproduced triplicates.

For the transfection experiments, plasmid DNA pEGFP-N1 (9  $\mu$ g/mL, 4.7 kb, molar mass 2.9 MDa, Clontech, Mountain View, CA) was added to the culture medium and the cells were irradiated at 60 mW for 35 ms. Targeted cells were imaged after 24–48 hours of incubation using Nikon Eclipse TE2000-S microscope equipped with a FITC HyQ filter (Chroma Technology, Bellows Falls, VT). The images of fluorescent cells were photographed using NIS-Elements BR software version 3.0 (Nikon Instruments, Melville, NY) with the exposure time of 3 seconds and the gain of 1.00X. The cells without laser irradiation were used as negative controls to assess the background auto-fluorescence.

### 3. RESULTS AND DISCUSSION

#### 3.1. Cell Survival with Varying Laser Parameters

The average laser power that can be used in the femtosecond laser optoporation experiments is critical and must be determined in advance. In general, the average laser power should be in a range that is low enough to avoid the cell damage but sufficient to induce perforation on the plasma membrane. The laser power and the exposure time at the threshold of the cell damage varies from one cell line to another. We tested the viability of HEK cells after laser irradiations at varying parameters to estimate the range of the laser power and the exposure time that the cells can tolerate. We used both direct physical observation of their morphology and differential staining using Trypan Blue to assess the viabilities of laser-treated cells. Cells were permanently damaged and died immediately after laser exposures at higher than 70 mW even if they are irradiated for a very short time (Fig. 2(a)). For the power range between 50–70 mW, the cells died only when the exposure time exceeded 50 ms. When the average laser power was set to 40–50 mW, some cellular morphological changes were observed such as membrane blebbing (“bubbles”) with the

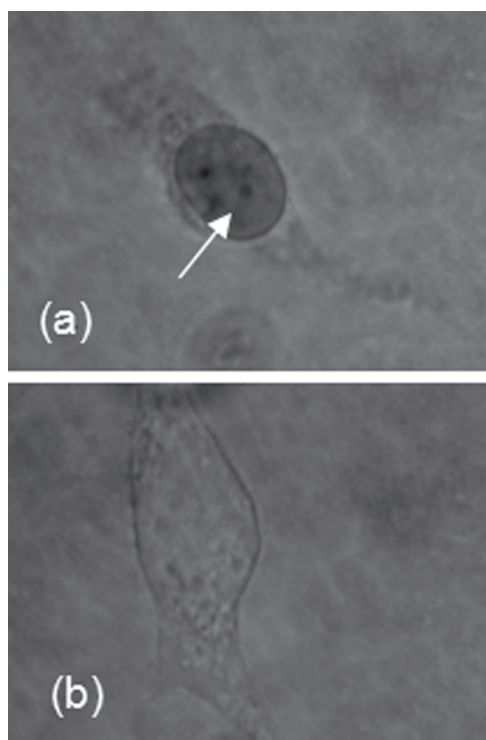


**Fig. 2.** Bright field images of laser-treated HEK cells: Trypan Blue (0.5%) was added to the culture medium 40 minutes after laser treatment to test cell-viability. Trypan Blue is a membrane-impermeable differential dye that stains dead cells but not live cells. (a) High laser exposure (power = 80 mW; exposure time = 10 ms) resulted in staining of the targeted HEK cell. Presence of Trypan Blue indicates that the integrity of the HEK plasma membrane has been compromised. (White arrow) (b) HEK cell survived after near-optimal laser exposure (power = 60 mW; exposure time = 30 ms).

exposure time exceeding 50 ms. However, when the laser irradiation time was reduced to the range of 20–40 ms, the temporary membrane blebbing healed shortly after the treatment and the irradiated cells survived (Fig. 2(b)). When the laser average power was reduced to less than 20 mW, no cellular change was observed even after a very long exposure time (100 ms).

#### 3.2. Optimization of Laser Conditions for Cellular Optoporation

We further optimized the parameters for cellular optoporation by monitoring the influx of a fluorescent indicator into the targeted cells. A  $4 \times 4$  square grid was fabricated on the bottom-side (outside) of the growth area (see Materials and Methods for details) to systematically compare multiple combinations of laser power and exposure time. Single HEK cells at the corners of each square grid were identified as targeted cells and cells adjacent to the targeted cells served as the control population. Cells were irradiated with varying exposure parameters in the presence of SYTOX Green reagent. SYTOX is a small molecule-based dye which is impermeable to the intact plasma membrane of live cells. Upon entering the cells, the dye binds to nucleic acids and produce fluorescence signal. Based on the threshold for cell survival estimated from the previous section, we fixed the laser power at 60 mW since this is the highest laser power that all tested cells were able to tolerate at the exposure time of less than 50 ms. The exposure time was varied between 30 ms and 40 ms. The optimal and most reproducible results were obtained from the laser exposures at 60 mW for 35 ms, indicated by the positive uptake of SYTOX by intact cells. Figure 3 shows a representative result of optoporation with these optimal parameters. An increase of fluorescence inside the cell was observed as a function of time, indicating successful perforation of the plasma membrane. The SYTOX dye mainly accumulated in the nucleus as expected.

As controls, no signs of dye uptake was observed by the adjacent non-treated cells, indicating that the laser exposure on the plasma membrane is required to change the membrane permeability (Fig. 3). Also, no change was observed when the laser focus was in the vicinity of the cell but not on the cell. The irradiated cells were negative to the Trypan Blue stain which verifies the recovery of membrane integrity and overall cell viability after laser treatment.

At the laser exposure time of 30 ms, the influx of SYTOX into the targeted cells was observed, however the intensity of the fluorescence (Fig. 4(d)) was decreased compared to Figure 3(f). This result indicates that the total amount of dye introduced into the cell was reduced at the exposure time of 30 ms compared to 35 ms.

Another often neglected experimental parameter is the location of laser focus on the cell-membrane. Force mapping using atomic force microscope (AFM) have demonstrated significant differences in properties of protruding

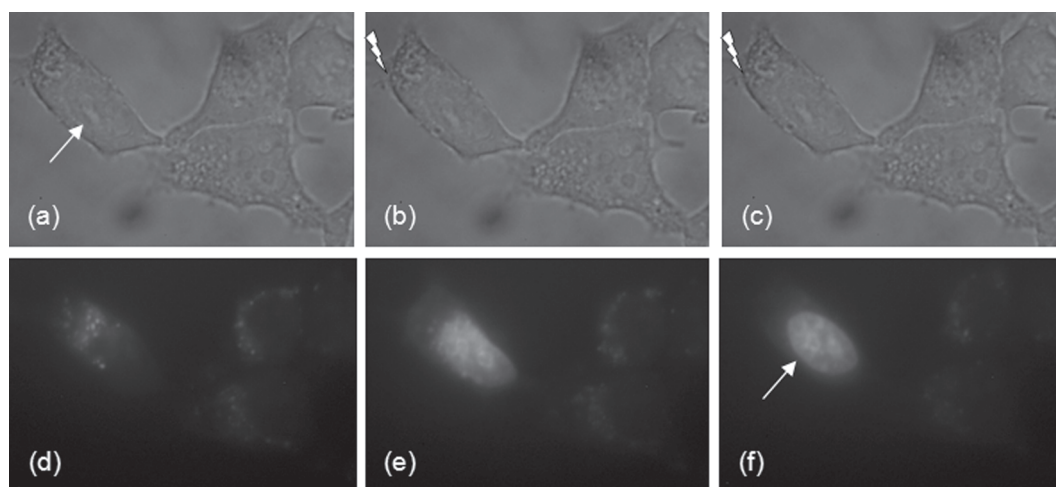


**Fig. 3.** Bright field images (a, b, c) and fluorescence images (d, e, f) of intact HEK cells after optoporation experiment in the presence of SYTOX dye. The position of the laser focal spot is marked by the lightning symbol. White arrow points to the targeted cell. Laser power = 60 mW; Exposure time = 35 ms. (a) (d) Before laser irradiation; (b) (e) Fluorescence is observed inside the HEK cell 10 min after laser optoporation; (c) (f) SYTOX stains only the nucleus of the cell, 20 min after optoporation.

and stable edges of 3T3 fibroblasts in culture.<sup>11</sup> Active edges of 3T3 cells are flatter (average heights = 0.4–0.8 mm) and are softer (elastic modulus = 4 kPa), while stable edges are thicker (average height = 2 mm) and stiffer (elastic modulus = 12 kPa). Optoporation experiments in this work also demonstrate differences in the protruding and stable edges of HEK cells (Fig. 4(c)). The successfully optoporated cell shown in Figure 4 was irradiated at a protruding edge with a laser power of 10 mW and a exposure time of 30 ms. To achieve optoporation of

Delivered by Ingenta to:  
Rice University, Fondren Library

stable edges of HEK cells, however the power had to be increased to 70 mW which resulted in deaths of most cells as described in the previous section. This result underscores the significance of choosing specific location on cell membrane while conducting optoporation experiments.

When the exposure time was increased to 40 ms at laser power 60 mW, membrane blebbing was observed within the target region indicating some cell damage regardless of whether the cell was irradiated at a stable edge (Figs. 5(a–c)) or a protruding edge (Figs. 5(d–f)). In most

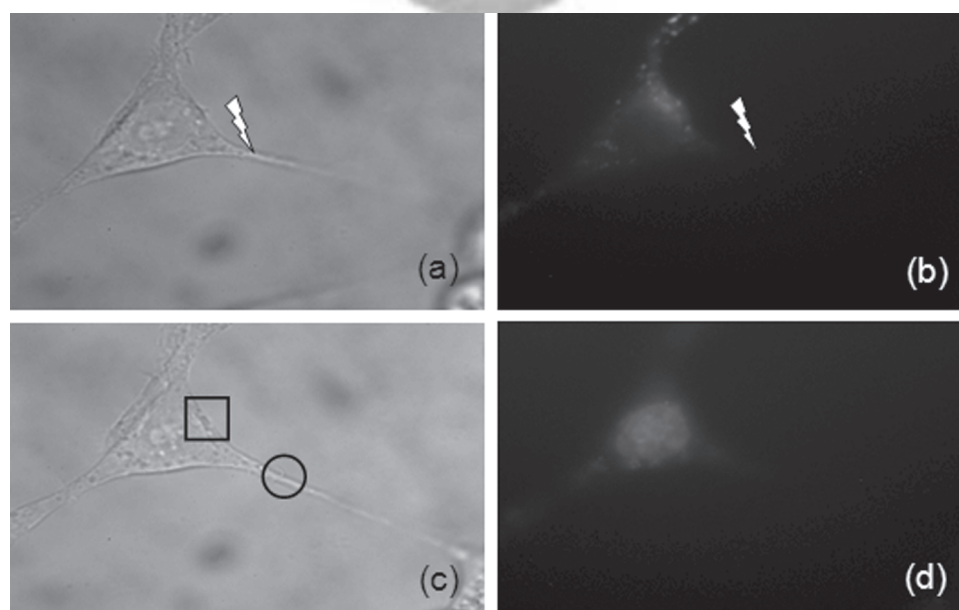


**Fig. 4.** Bright field (a, c) and fluorescence images (b, d) of an HEK cells after laser treatment in the presence of SYTOX dye at a reduced exposure time than the optimal (laser power = 60 mW; exposure time = 30 ms). The position of the laser focal spot is marked by the lightning symbol. (a, b) 10 min post-exposure (c, d) 20 min post-exposure. Fluorescence labeling the nucleus was observed 20 min after laser optoporation. Square in (c) = stable edge; circle in (c) = protruding edge.

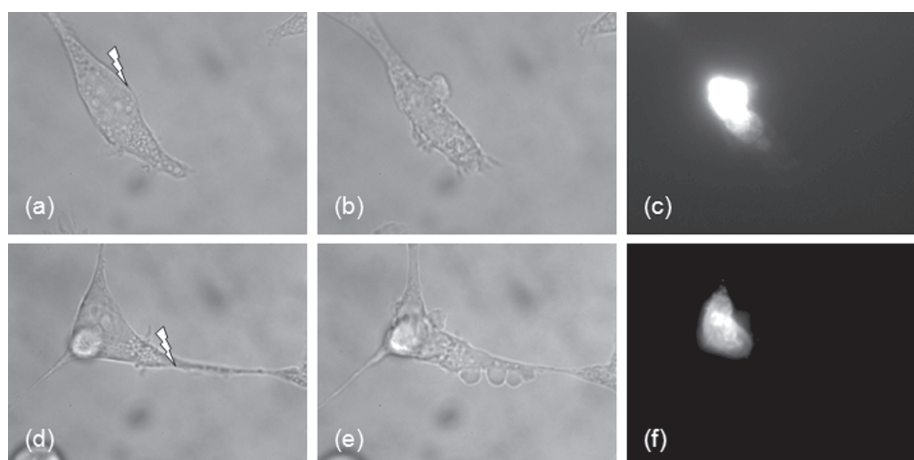


**Fig. 5.** Morphological changes of two HEK cells (laser power = 60 mW; exposure time = 40 ms) post-irradiation at the marked positions: (a, d) 0 min after laser treatment; (b, e) 10 min after laser treatment. Excessive local swelling of the plasma membrane was observed in both cells. (c, f) 20 min after laser treatment. SYTOX dye is seen inside the cell, however it does not bind to only the nucleus. Both cells were determined to be non-viable based on Trypan Blue staining.

cases, when 2 or more bubbles are present for longer than 10 min post-exposure, the cell membrane is compromised based on the Trypan Blue staining. However, when the size of the bubble is about 1 micrometer or less in diameter, most cells recover within 10 min of laser treatment with no signs of membrane damage. A summary of results are shown in Figure 6.

### 3.3. Transfection of HEK Cells by Femtosecond Laser-Assisted Cellular Optoporation

We used the optimized laser parameter (laser power = 60 mW; exposure time = 35 ms) to perform DNA transfection experiments with HEK cells. Cells were irradiated in the presence of plasmid DNA pEGFP-N1 in the culture medium and then returned to the incubator. Targeted cells were identified by using the grid as described in the methods section 24–48 hours post-treatment. Positive expression of GFP in the irradiated cells and their daughter cells after cell division indicates that the plasmid DNA was successfully introduced into the cell interior by optoporation treatment (Fig. 7). No fluorescence was observed in the surrounding cells not exposed to the laser.

### 3.4. Simulation of Femtosecond Laser Ablation of Plasma Membrane

Laser intensity plays an important part in determining optimum pore formation on cell membrane during optoporation.<sup>10</sup> Laser beam with higher than threshold energy level will disintegrate cells. To better understand the laser energy produced during the optoporation process, we simulated the near infrared (NIR) femtosecond laser ablation process.

The parameters of the laser we use (Vitesse, Coherent Inc. Santa Clara, CA) were as follows: wavelength  $\lambda = 800$  nm; repetition rate = 80 MHz;

pulse duration = 100 femtoseconds. The numerical aperture (NA) of the oil immersion lens (Fluar, Carl Zeiss MicroImaging, Inc. Thornwood, NY) we used to focus the laser was 1.3. We use water as the aquatic medium in the simulation to simplify the calculation, since optical properties of the culture media we used (Dulbecco's Modified Eagle's Medium, no phenol red, Invitrogen Inc., Carlsbad, California) are similar to those of water.

Vogel et al. have demonstrated that a high repetition rate femtosecond laser ablates biological material by generating low density plasma within the focus.<sup>19</sup> The low density plasma is formed by multiphoton ionization process. Single photon effect (linear absorption) is neglected for NIR laser interaction with biological material because biological material is almost transparent (optical window) at NIR region.

To obtain the plasma (free electron) distribution within the focal volume, we need to calculate the laser irradiance distribution first. Born et al. revealed that the laser focal region had a shape of ellipsoid.<sup>4</sup> We approximate the length of the short axis of the ellipsoid  $d$  by the diameter of the Airy disc.

$$d = 1.22 \frac{\lambda}{\text{NA}} \quad (1)$$

For our case,  $\lambda = 800$  nm,  $\text{NA} = 1.3$ , so the short axis  $d$  is 750 nm. The ratio of the long axis and short axis for the ellipsoid is revealed by Gril et al.<sup>5</sup>

$$\frac{l}{d} = \frac{\sqrt{3 - 2\cos(\alpha) - \cos(2\alpha)}}{1 - \cos(\alpha)} \quad (2)$$

Where  $\alpha$  is the opening angle for the objective lens and  $l$  is the length of long axis. We use the definition of NA to calculate  $\alpha$ . For  $\text{NA} = 1.3$  and refractive index of water = 1.333,  $\alpha = 77.2^\circ$ . So  $l/d = 2.4$  and  $l = 1800$  nm.

Gaussian function is used to simulate the distribution of laser irradiance within the focal region. To simplify the

		Laser Power		
		50 mw	60 mw	70 mw
Laser exposure time	30 ms		<ul style="list-style-type: none"> <li>• SYTOX dye labels nucleus</li> <li>• Weak fluorescence signal</li> <li>• No bubble formation</li> <li>• Cell viable</li> </ul>	
	35 ms	<ul style="list-style-type: none"> <li>• No fluorescence signal</li> <li>• No bubble formation</li> <li>• Cell viable</li> </ul>	<ul style="list-style-type: none"> <li>• SYTOX dye labels nucleus</li> <li>• Strong fluorescence signal</li> <li>• Some bubble formation</li> <li>• Cell viable</li> </ul>	<ul style="list-style-type: none"> <li>• Strong fluorescence signal</li> <li>• Cell blebbing</li> <li>• Cell non-viable</li> </ul>
	40 ms		<ul style="list-style-type: none"> <li>• SYTOX dye labels nucleus</li> <li>• Strong fluorescence signal</li> <li>• Excessive bubble formation</li> <li>• Cells non-viable</li> </ul>	

Fig. 6. Summary of femtosecond laser-optoporation results using HEK cell line.

calculation, we use its corresponding time-averaged intensity distribution, which is given by Eq. (3). Then we use  $Q(I(0))$  to represent the free electron density at the center of the ellipsoid and obtain Eq. (5).

$$I(r, z) = I(0) \exp \left[ -2 \left( \frac{r^2}{a^2} + \frac{z^2}{b^2} \right) \right] \quad (3) \quad Q(r, z) = Q[I(0)] \exp \left[ -2k \left( \frac{r^2}{a^2} + \frac{z^2}{b^2} \right) \right] \quad (5)$$

$I(0)$  is the irradiance at the center of the beam at the waist,  $a = d/2$ , and  $b = l/2$ .

We adopt Vogel et al.'s assumption that the free electron density is proportional to  $I^k$ , while  $k$  is the number of photons required to initiate multiphoton ionization.<sup>19</sup> So the distribution of free electron is derived as Eq. (4).

$$Q(r, z) \propto \left\{ I(0) \exp \left[ -2 \left( \frac{r^2}{a^2} + \frac{z^2}{b^2} \right) \right] \right\}^k \quad (4)$$

Since the band-gap energy of water is 6.5 eV and the photon energy of 800 nm laser is 1.56 eV, 5 photons are required to be sequentially absorbed to ionize water. So  $k = 5$  in Eq. (5).

The normalized distribution of laser irradiance and free electron density are calculated by Matlab® (Mathworks Inc.) and demonstrated in Figure 8. The results show that the free electron distribution is much narrower than the laser irradiance, which implies that the transient

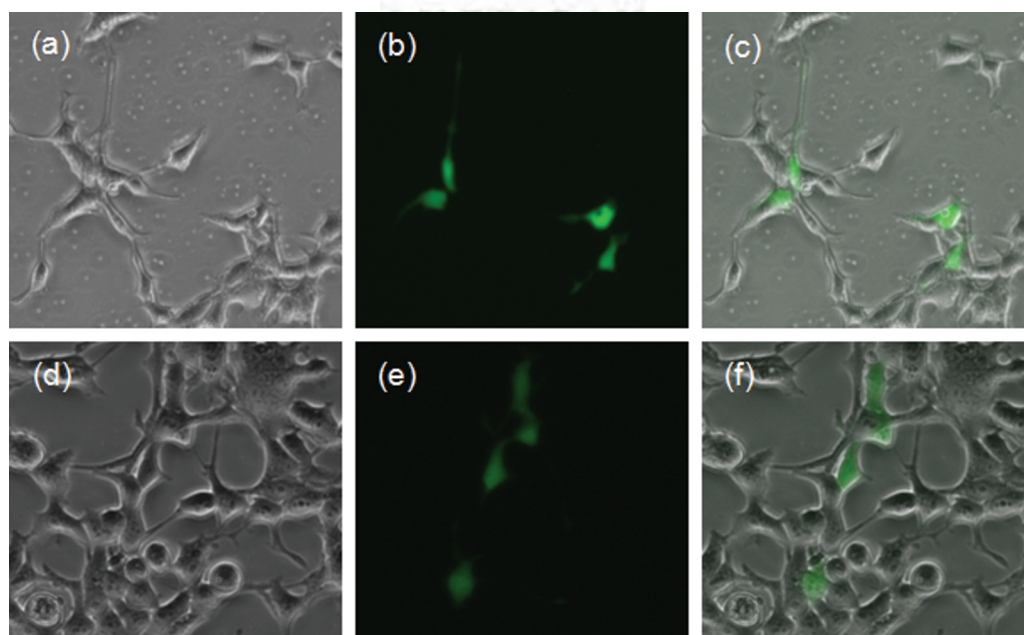
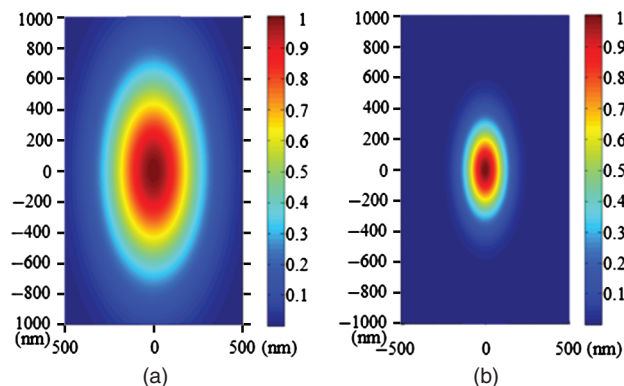


Fig. 7. Transfection of HEK cells using femtosecond laser. Four HEK cells were optically transfected with plasmid DNA pEGFP-N1 and analyzed 24–48 hours post treatment. (a, d) Brightfield images. (b, e) Fluorescence images. (c, f) Superimposed images.



**Fig. 8.** (a) The normalized laser irradiance (unit:  $\text{W}/\text{cm}^2$ ) distribution in the focal point. It demonstrates that the irradiance distribution has an ellipsoidal shape, in which the highest irradiance is in the center and the irradiance exponentially decays from inner layer to outer layer. The color bar is the scale of normalized laser irradiance, in which 1 is the normalized irradiance at the center. (b) The normalized free electron (plasma) distribution (unit:  $\text{cm}^{-3}$ ) in the focal point. It shows that the plasma distribution has the same shape as the irradiance distribution but much smaller size, which is the reason why femtosecond laser is able to create a hole smaller than the size of its focal point on cell membrane. The color bar is the scale of normalized free electron density, in which 1 is the normalized density at the center.

perforation can even be smaller than the size of the laser focal volume. Using this result, other researchers can calculate the laser irradiance and electron density distribution by simply changing the variables (wavelength, numerical aperture of objective lens etc.) according to their specific laser set-up.

**Acknowledgment:** This work is supported by grants to S.C. from the Office of Naval Research and the National Science Foundation.

## References and Notes

- B. Alberts, A. Johnson, J. Lewis, M. Raff, K. Roberts, and P. Walter, *Molecular Biology of the Cell*, Garland Science, New York (2002).
- H. Andersson and A. van den Berg, *Microtechnologies and nanotechnologies for single-cell analysis*. *Curr. Opin. Biotechnol.* 15, 44 (2004).
- J. Baumgart, W. Bintig, A. Ngezahayo, S. Willenbrock, H. Murua Escobar, W. Ertmer, H. Lubatschowski, and A. Heisterkamp, Quantified femtosecond laser based opto-perforation of living GF5HR-17 and MTH53 a cells. *Opt. Express* 16, 3021 (2008).
- M. Born and E. Wolf, *Principles of optics: Electromagnetic theory of propagation, Interference and Diffraction of Light*, Pergamon Press, Oxford, New York (1970).
- S. Grill and E. H. K. Stelzer, Method to calculate lateral and axial gain factors of optical setups with a large solid angle. *J. Opt. Soc. Am. A* 16, 2658 (1999).
- I. Hapala, Breaking the barrier: Methods for reversible permeabilization of cellular membranes. *Crit. Rev. Biotechnol.* 17, 105 (1997).
- S. K. Koester and W. E. Bolton, Intracellular markers. *J. Immunol Methods* 243, 99 (2000).
- M. Lei, H. Xu, H. Yang, and B. Yao, Femtosecond laser-assisted microinjection into living neurons. *Journal of Neuroscience Methods* 174, 215 (2008).
- P. A. Norton and C. J. Pachuk, Methods for DNA introduction into mammalian cells. *Gene Transfer and Expression in Mammalian Cells*, edited by S. C. Makrides, Elsevier Science, Amsterdam, BV (2003), pp. 265–277.
- C. Peng, R. E. Palazzo, and I. Wilke, Laser intensity dependence of femtosecond near-infrared optoinjection. *Phys. Rev.* 75, 041903 (2007).
- C. Rotsch, K. Jacobson, and M. Radmacher, Dimensional and mechanical dynamics of active and stable edges in motile fibroblasts investigated by using atomic force microscopy. *Proceedings of the National Academy of Sciences of the United States of America* (1999), Vol. 96, pp. 921–926.
- C. E. Sims and N. L. Allbritton, Analysis of single mammalian cells on-chip. *Lab. Chip.* 7, 423 (2007).
- D. J. Stevenson, F. J. Gunn-Moore, P. Campbell, and K. Dholakia, Single cell optical transfection. *Journal of the Royal Society Interface* 7, 863 (2010).
- F. Stracke, I. Rieman, and K. Konig, Optical nanoinjection of macromolecules into vital cells. *Journal of Photochemistry and Photobiology B: Biology* 81, 136 (2005).
- U. K. Tirlapur and K. Konig, Cell biology: Targeted transfection by femtosecond laser. *Nature* 418, 290 (2002).
- A. Uchugonova, K. Konig, R. Bueckle, A. Isemann, and G. Tempea, Targeted transfection of stem cells with sub-20 femtosecond laser pulses. *Opt. Express* 16, 9357 (2008).
- C. J. Van Noorden, Imaging enzymes at work: Metabolic mapping by enzyme histochemistry. *J. Histochem. Cytochem.* 58, 481 (2010).
- K. Vikram, P. Jason, and Y. Abdulhakem, Reversible permeabilization using high-intensity femtosecond laser pulses: Applications to biopreservation. *Biotechnology and Bioengineering* 92, 889 (2005).
- A. Vogel, J. Noack, G. Hüttman, and G. Paltauf, Mechanisms of femtosecond laser nanosurgery of cells and tissues. *Appl. Phys. B: Lasers and Optics* 81, 1015 (2005).
- Y. Zhang and L. Yu, Single-cell microinjection technology in cell biology. *Bioessays* 30, 606 (2008).

Received: 10 October 2010. Revised/Accepted: 16 February 2011.